



## Stability of S-layer proteins for electrochemical nanofabrication

Alvaro Presenda<sup>a</sup>, Daniel B. Allred<sup>b</sup>, François Baneyx<sup>a</sup>,  
Daniel T. Schwartz<sup>a,b</sup>, Mehmet Sarikaya<sup>a,b,\*</sup>

<sup>a</sup> Department of Chemical Engineering, University of Washington, Seattle, WA, United States

<sup>b</sup> Department of Materials Science and Engineering, University of Washington, Seattle, WA, United States

Received 27 October 2006; received in revised form 13 January 2007; accepted 8 February 2007

### Abstract

Crystalline cell surface layer proteins (S-layers) can be used in electrochemical fabrication to create nanoscale arrays of metals and oxides on surfaces so long as the proteins maintain their long-range order during processing. We have explored the stability of the HPI layer protein (the S-layer protein from the microorganism *Deinococcus radiodurans*) adsorbed onto platinum surface after immersion in sulfuric acid or sodium hydroxide electrolytes ranging in pH from 0 to 14 over time periods ranging from 1 to 1000 s. Topographic data obtained by atomic force microscopy (AFM) was used to characterize the protein stability, judged by its retention of long-range order after immersion. The compiled data revealed that, under these solution conditions and in this environment, the HPI layer protein has a dose-dependent structural stability “envelope” in the acidic range from  $1 < \text{pH} < 4$ . The protein retains its long-range order up to 1000 s from pH 4 to 11, and has a sharp stability edge between pH 12 and 13. Interestingly, the more stringent requirement of stability (*i.e.*, retention of long-range order) defined in the context of electrochemical fabrication for this protein narrowed the window of stability in pH and time when compared to previous stability studies reported for this protein.

© 2007 Published by Elsevier B.V.

**Keywords:** *Deinococcus radiodurans*; Protein stability; Atomic force microscopy; pH stability study; S-layer proteins; Electrodeposition; HPI layer

### 1. Introduction

Bacterial cell surface layer proteins are becoming increasingly popular systems for organizing and templating the synthesis of nanomaterials [1–9]. These proteins are generically categorized as the *paracrystalline* outer cell wall protein found enveloping cells of many microbiological species [10]. They are well known for having a high degree of order even when removed from the cell surface, and having high tolerance to harsh chemicals and temperature variability [11].

Previously, we have demonstrated that S-layer proteins can serve as masks for electrochemical fabrication of metal and semiconductor nanoarrays [8]. Protein-based electrochemical fabrication allows smaller and higher density packing of periodic elements than lithography-based methods widely used in integrated circuit fabrication technology. Initial results relied on

electrolyte formulations from the literature or those available commercially. The quality of the resulting patterned materials varied from exceptional, in the case of cuprous oxide, to poor, for platinum, to non-existent, for copper. The initial hypothesis for these varied results was based primarily on poor optimization of the electrodeposition process, which can be finely tailored to satisfy the high nucleation density required for the electrochemical fabrication of individual units at a density on the order of  $10^{12} \text{ cm}^{-2}$  on the work surface. However, an alternative hypothesis for poor pattern transfer could be that the various electrolytes may disrupt the long-range order of the S-layer protein of *D. radiodurans* (also known as the HPI layer, or the hexagonally packed intermediate layer, protein). This alternative hypothesis was initially rejected owing to the extensive characterization of this protein [12,13] which indicated a broad stability over time scales (16 h or greater) far exceeding that needed for electrochemical fabrication.

An early study on the HPI layer stability used precipitation as an indicator that the proteins survived exposure to various aggravating conditions [12]. However, precipitation alone does not differentiate between HPI layer proteins that have a long range ordered nanostructure (desirable for electrochemical

\* Corresponding author at: Department of Chemical Engineering, University of Washington, Seattle, WA, United States. Tel.: +1 206 543 0724; fax: +1 206 543 6381.

E-mail address: [sarikaya@u.washington.edu](mailto:sarikaya@u.washington.edu) (M. Sarikaya).

fabrication) from disordered HPI layer protein aggregates large enough to precipitate. Later stability studies used transmission electron microscopy in conjunction with heavy metal staining [13] to examine the fine structure of the protein, a more stringent test which may be more useful for electrochemical fabrication. However, as the degradation of the HPI layer protein was tested on a time scale of several hours to overnight, and short contact times are of much greater interest, this information may be unnecessarily conservative for fabrication purposes.

Here, we explore the temporal stability of the HPI layer protein adsorbed on surfaces as a function of electrolyte pH (one of the key variables in formulating baths for electrochemical fabrication). The figure of merit for this protein is its ability to retain its long-range order upon exposure to the electrolyte. This refined definition narrows the window of stability of the *D. radiodurans* HPI layer protein when compared to the window of stability against other modes of degradation such as proteolysis or acid hydrolysis, but it permits a rational approach to formulating an electrolyte to achieve successful pattern transfer. We demonstrate the value of this approach by re-examining copper electrodeposition through the HPI layer proteins, a process that previously failed when using conventional electrolytes.

## 2. Experimental methods

### 2.1. Protein preparation

Intact 2D HPI-layer protein sheets were prepared as previously described [8], using methods adapted from the work of Baumeister et al. [14]. Briefly, A 1 L culture of *D. radiodurans* SARK (ATCC 35073) was grown to early stationary phase in TGY medium (0.3% tryptone/0.1% glucose/0.5% yeast extract) and washed in deionized water two times and finally resuspended in 2% sodium dodecyl sulfate (SDS). The cell suspension was shaken for 2 h in a rotary shaker at 60 °C. Cells were sedimented at  $2200 \times g$  for 15 min and discarded. The supernatant was centrifuged at  $18,000 \times g$  for 45 min and the protein pellet was resuspended in 5% SDS. This process was repeated until no solid material was visible at the bottom of the tube after centrifugation at  $2200 \times g$ . SDS-polyacrylamide gel electrophoresis [15] revealed a protein band at about 100 kDa as well as sub-fragments previously identified to be strain-specific cleavage patterns from an extracellular protease [16]. The final volume of the suspension was brought to 3 mL, corresponding to an estimated S-layer protein concentration of  $1 \text{ mg mL}^{-1}$ , which was estimated by the Bradford assay [17] using bovine serum albumin (BSA, Sigma–Aldrich) as a standard and a protein sample resuspended in deionized water. The stock sample for all experiments was diluted into 5% SDS to about  $0.25 \text{ mg mL}^{-1}$  for routine use.

### 2.2. Protein adsorption

Protein adsorption on surfaces was performed as previously described [8], and summarized here for the reader's convenience. For atomic force microscopy (AFM), grade V-4 muskovite mica (Structure Probe, Inc.) was mounted onto steel AFM pucks. The

mica surface was cleaved using Scotch® tape and immediately sputter-coated in a Gatan PECS system with 10 nm of platinum based on *in situ* quartz crystal microbalance monitoring. For transmission electron microscopy (TEM), platinum-coated gold TEM grids (Structure Probe, Inc.) were used.

For AFM, 15–20  $\mu\text{L}$  of stock protein suspension was used, whereas 2–3  $\mu\text{L}$  was used for TEM imaging. The protein was applied on the surface by pipette and allowed to sit for about 30–60 s. The surface was then gently rinsed by repeated immersion in deionized water and either dried under argon for AFM analysis or wicked dry with a wipe for TEM experiments.

### 2.3. Sample preparation

Test solutions of sulfuric acid or sodium hydroxide were prepared by adding concentrated (10 M) sulfuric acid or sodium hydroxide to deionized water. The pH was monitored using high-resolution pH indicator strips (colorpHast®, EM Science). The protein-coated surface was exposed to a given test solution for a predetermined time and immediately blown dry under argon. The surface was then rinsed by repeated immersion in deionized water and dried under argon.

### 2.4. Atomic force microscopy (AFM)

AFM was performed on a Nanoscope® III AFM under Tapping Mode® conditions using amplitude feedback control. Linear scans rates were typically  $0.8\text{--}1.2 \mu\text{m s}^{-1}$ . Probes were aluminum-coated Pointprobe® Plus (Nanosensors) SPM probes with a typical resonance frequency of 250–350 kHz and a nominal tip radius of less than 10 nm. Lateral size bars on images are based on calibrations with diffraction grating standards and are accurate to within 1%.

### 2.5. Transmission electron microscopy (TEM)

TEM was performed on a Philips 420 TEM ( $C_s \sim 1.3 \text{ mm}$ ) at 120 kV accelerating voltage using a tungsten filament. No objective aperture was used. Electron diffraction was used to verify the material's crystal structure by simulating it with a powder diffraction analysis. The effective camera length was calibrated by an aluminum foil standard. Size bars on images are based on calibrations with diffraction grating replicas and are estimated to be accurate to within 5%.

### 2.6. Copper electrodeposition

Electrodeposition was performed in a quiescent, three-electrode, single compartment cell operating at room temperature. The working electrode (cathode) was composed of the protein-adsorbed platinum-coated gold TEM grid held by self-closing anti-capillary tweezers at an acute angle to the electrolyte surface. The counter electrode (anode) was a piece of platinum foil angled nearly parallel to the working electrode. The reference electrode was a saturated calomel electrode (SCE) and all voltages are reported as cathode potentials with respect to the SCE.

138 Electrolytes of two types were prepared: a 0.5 M sulfuric  
139 acid/0.5 M cupric sulfate electrolyte (pH ~ 0) and a comparable  
140 bath of 0.5 M sodium sulfate/0.5 M cupric sulfate, using sulfuric  
141 acid to adjust the pH to 3.

### 142 3. Results and discussion

143 The S-layer protein of *D. radiodurans* (HPI) can be purified  
144 as intact 2D protein “sheets”. The two faces of the sheet have  
145 different characteristics. Upon adsorption to surfaces, either face  
146 of the sheet may be exposed; for labelling purposes, one face  
147 will be referred to as face “A” (Fig. 1A) and the other as face  
148 “B” (Fig. 1B) in this article. Inspection of the images in Fig. 1  
149 shows that, whereas the periodicity is the same for either “A”  
150 or “B” faces, the topography is greatly different. On a routine  
151 basis, the hexagonal arrangement of face “B” is rarely resolved,  
152 while face “A” can in nearly all cases. Because the goal of this

153 study is to evaluate long-range order, there was a real danger of  
154 mislabeling an intact protein sheet as disordered because face  
155 “B” was exposed to the tip. To avoid this error, a standardized  
156 “blind trial” protocol was developed (Fig. 2A and B).

157 The first step consists in scanning at low enough resolution  
158 (fewer scans along the slow scan axis) so that the pattern –  
159 whether it is present or not – cannot be observed, but the outline  
160 of protein sheets are still visible with height steps corresponding  
161 to single, double, or additional protein layers (Fig. 2A). Having  
162 multiple height steps in the scan maximizes the likelihood that  
163 in the field of view, both faces of the protein sheet are going  
164 to be exposed to the tip. Once a protein fragment is identified,  
165 it is selected as a candidate for a higher resolution scan  
166 (Fig. 2B). An important feature in the high-resolution scan is  
167 the imaging of the platinum-coated mica background, which  
168 provides a reproducible 2–5 nm cobblestone structure. The plat-  
169 inium surface itself, therefore, serves as an internal resolution

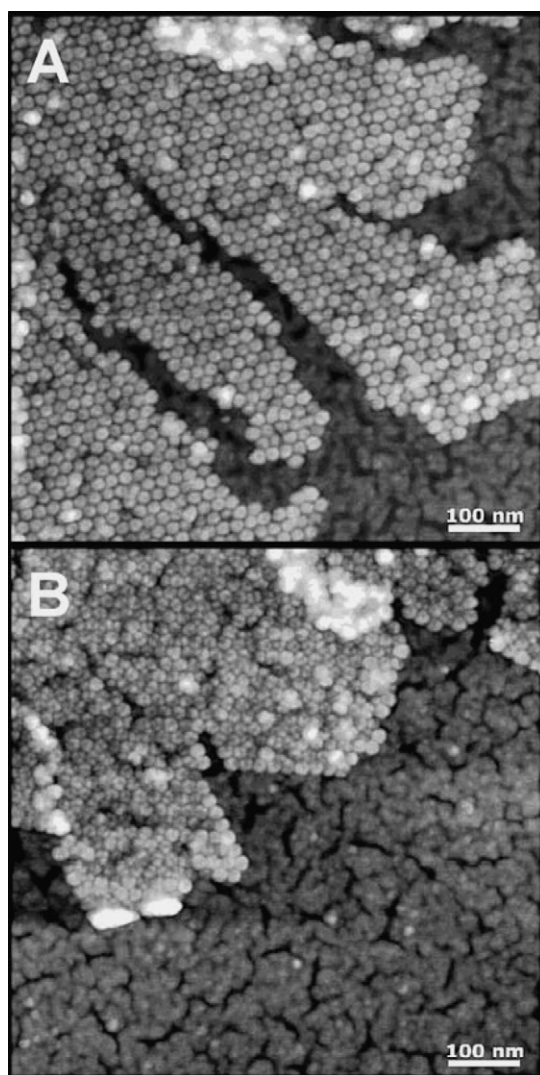


Fig. 1. Atomic force microscope image pair of S-layer protein cell wall fragments from *Deinococcus radiodurans* adsorbed on platinum coated mica revealing the topography of both orientations. Protein sheets will have their faces designated as face “A” (A) or face “B” (B). Proteins are about 5–6 nm high with respect to the platinum surface.

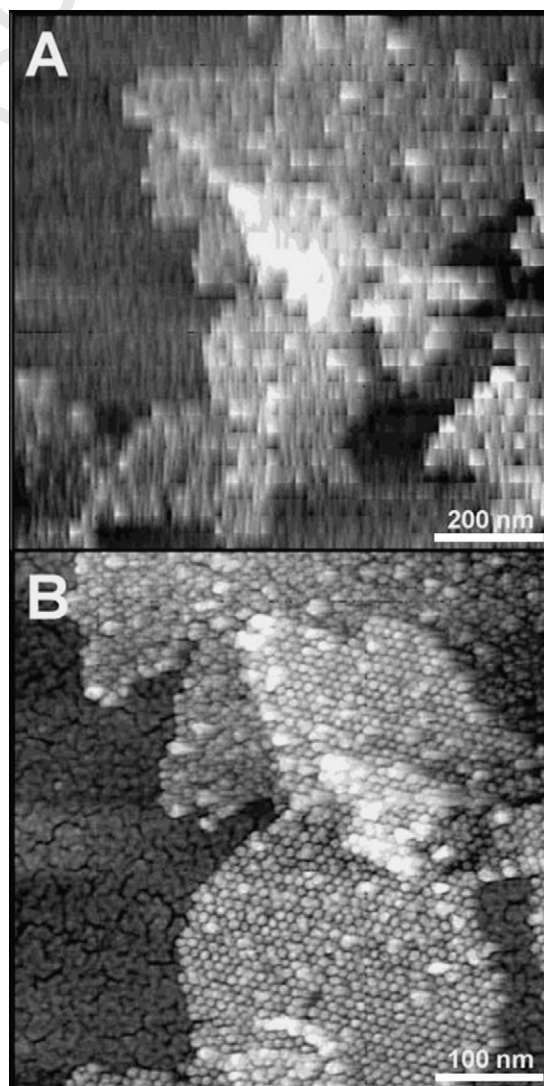


Fig. 2. Standardized protocol for a single imaging experiment in which adsorbed HPI protein has been exposed to a sample electrolyte. A low-resolution scan (A) is used to search for a characteristic region containing protein sheets with multiple height information. A subsequent high-resolution scan (B) is used to examine protein pattern quality.

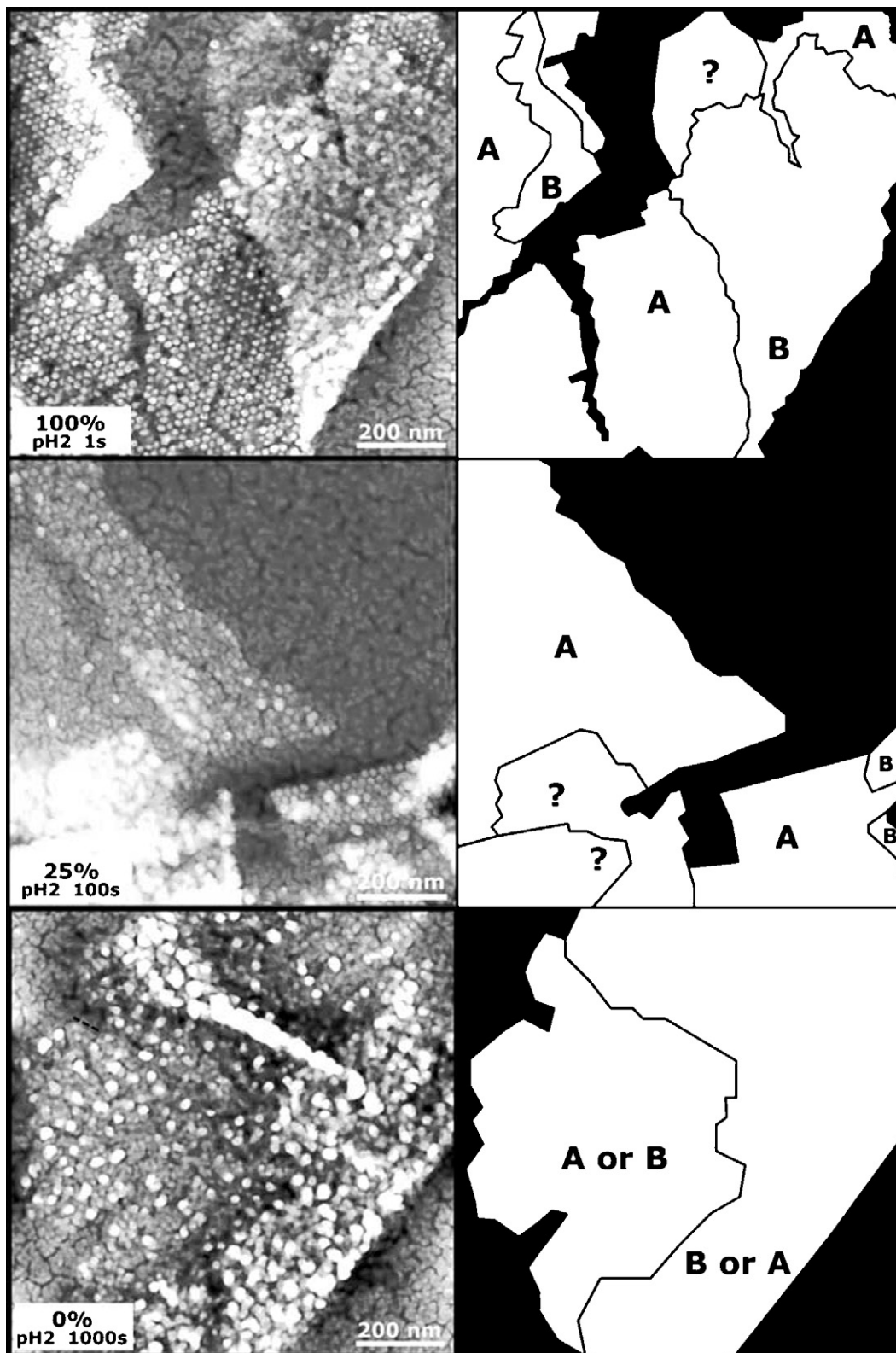


Fig. 3. Sample AFM data illustrating how quality was assessed. Images of multiple protein sheets obtained (left) and region outlining a protein sheet (as indicated in schematics on the right) were identified. Only sheets exposing face "A" can be used for evaluation except under conditions of totally disordered (0% quality). If all proteins in the same sheet are ordered the quality is ranked 100%. Intermediate values were ranked into quartiles by judging the size of the region containing hexagonal order relative to the size of the entire sheet exposing the same face. Conditions and the assigned quartile values (for the particular image shown) are indicated in the lower left of the image.

standard. If the platinum background cannot be imaged clearly, the image is not used for analysis and the AFM tip is replaced. In summary, the low-resolution scan allows image collection objectively without bias towards obtaining high quality data *a priori*. The need to have multiple protein layers in the field of view is essential to provide proteins exposing both faces to the tip, because one face could be easily mistaken for disordered protein.

Fig. 3 illustrates how the quality of a protein sheet was assessed after exposure to a given experimental condition. Shown are a series of sample AFM images taken after exposure of adsorbed HPI layer proteins to a sulfuric acid solution at pH 2 for 1, 100, and 1000 s. Proteins constituting a face are outlined and labelled as either face “A”, face “B”, or “?” if undeterminable. Only face “A” can be reliably used to evaluate quality as explained above. The quality of the protein sheet was estimated by ranking the images into quartiles from unflawed (100%) to totally disordered (0%). Intermediate values were estimated by the amount of protein lattice structure which could be discerned relative to the size of the entire sheet exposing the same face. More data was taken in the important “boundary” zone where variability was greatest. As protein sheets that are totally disordered (quality = 0%) have no determinable face, 0% can be assigned only when there is a clear fold of a protein resulting in a double step height from a height trace across the sheet so that regardless of which face is exposed, both faces must be present in the same image.

Fig. 4 shows the “phase diagram” of the complete HPI layer protein stability obtained from repeated experiments. The numbers in the spaces represent the total number of samples used for the particular test. Most data collection was focused on identifying the “boundary” of the stability envelope, where the transition occurs from useful protein to useless protein. Once identified, the rest of the diagram was filled in based on extrapolation or interpolation around the well-established data. Additionally, control experiments with 1 M sodium sulfate showed that the loss of long-range order primarily results from the acidity or basicity of the medium. Also, if ionic strength or a particular salt plays a

role in the degree of order, this happens so in a manner that couples with the pH of the solution. A worthwhile point to mention here is that, though this study did not extend out to many hours, under all conditions tested, protein sheets can still be found in abundance on the surface, whether disordered or not.

Fig. 4 provided the information needed to reformulate the copper electrolyte to fall within the envelope of the HPI layer stability. Of course, the pH value is not the only electrolyte component that may impact the stability of a given protein; therefore, Fig. 4 provides valuable guidance, though it does not ensure success. Only a specific study with all electrolyte components present could test a “point” in electrolyte formulation space. Fig. 5 shows TEM results before and after pH stability information was used to optimize the use of the HPI layer protein as a mask for the electrochemical fabrication of copper nanoparticles. In the previous work [8], we have shown that the HPI layer protein is an effective mask for the electrochemical fabrication of metal and metal oxide nanopatterns on surfaces. However, at that time it was not clear why the technique would not work for copper, an important material in the integrated circuit industry, and perhaps the most well studied metal for electrodeposition.

In the original experiments (unpublished), the use of a simple electrolyte consisting of 0.5 M sulfuric acid and 0.5 M cupric sulfate electrolyte (a common copper electrolyte) consistently failed to produce nanostructured films of copper. However, under these conditions, geometric patches of missing electron-density were observed, suggesting that electrodeposition did not successfully proceed through the S-layer protein mask (Fig. 5A). A pH test of the electrolyte revealed that the pH level was between 0 and 1. Although the fabrication is complete within 3–5 s, the data from Fig. 4 indicates that the integrity of the S-layer protein at such a low pH is entirely lost in the first seconds of exposure. The original experiments with copper were performed without the availability of Fig. 4 as a guide.

Fig. 4 provides a guideline for reformulating an electrolyte to fall within the stability of the protein. This will be especially important for simple metal electrolytes as they are generally quite acidic. To verify that the loss of HPI order was responsible

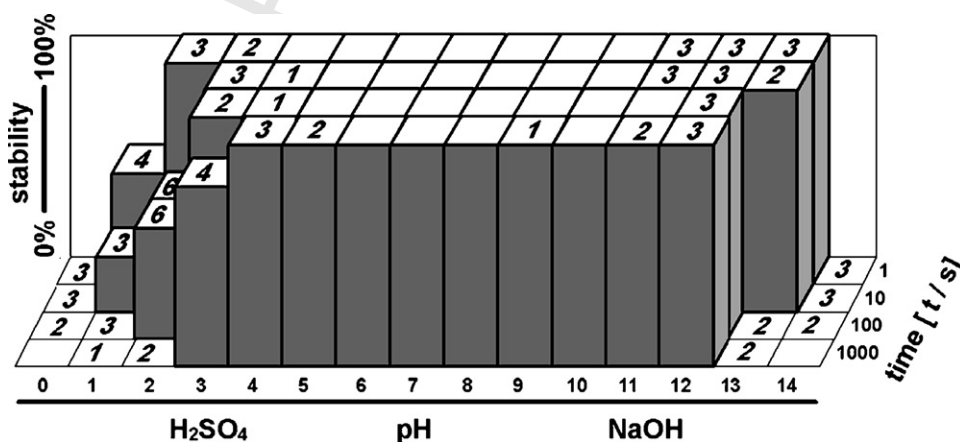


Fig. 4. The *D. radiodurans* S-layer protein stability “envelope” for electrochemical fabrication with respect to pH. Measurements were repeated until outliers were insignificant or did not occur and were performed most repeatedly along the “boundaries” of the stability envelope where quality of the protein crystal was neither 0% nor 100%. Numbers in the squares indicate number of repetitive measurements. Where numbers are missing, data was interpolated or extrapolated based on neighboring values. Error should be considered to be within one quartile of the values shown, and pH should be considered accurate to within 1 unit.

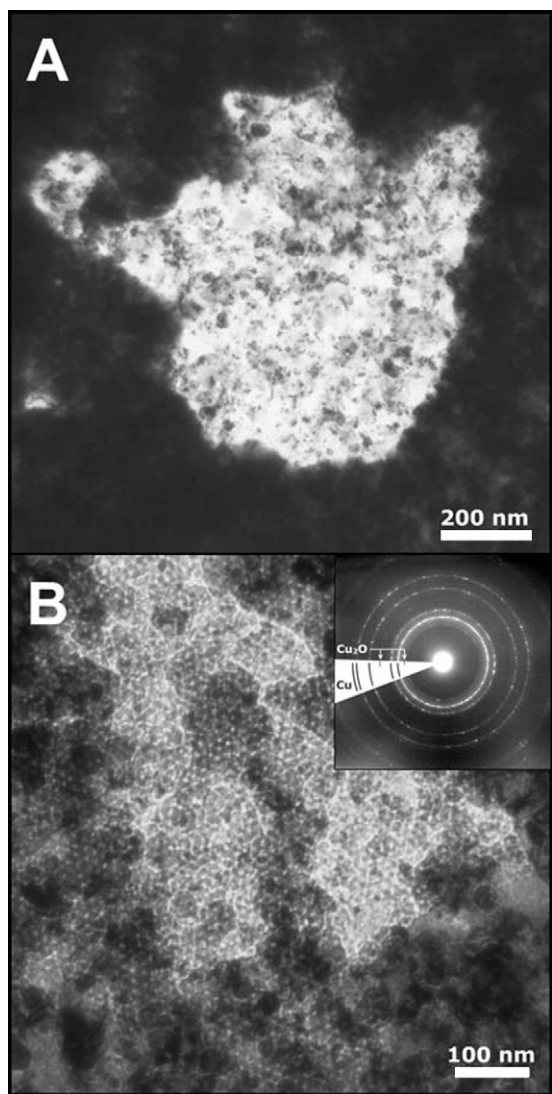


Fig. 5. Transmission electron micrographs of copper electrodeposited for 3 s at  $-300$  mV vs. SCE through S-layer proteins of *D. radiodurans* adsorbed onto platinum-coated gold TEM grids using electrolytes (A)  $0.5$  M  $\text{H}_2\text{SO}_4/0.5$  M  $\text{CuSO}_4$  at pH 0 and (B)  $0.5$  M  $\text{Na}_2\text{SO}_4/0.5$  M  $\text{CuSO}_4$  adjusted to pH 3 with  $\text{H}_2\text{SO}_4$ , showing the lack of and the presence of hexagonally structured electron dense material, respectively. Electron diffraction studies (inset of B) showed the electron dense material to be copper (with a trace of cuprous oxide, as expected for an oxidizable metal).

for the inability to fabricate copper nanopatterns, an electrolyte similar to the original one was prepared, except that the protons would be exchanged for sodium ions to keep the ionic strength of the electrolyte constant, *i.e.*,  $0.5$  M sodium sulfate and  $0.5$  M cupric sulfate adjusted to pH 3. This pH was chosen because it is a good compromise between the performance of protein and the electrochemistry where the protein should be able to survive for  $100$ – $1000$  s of exposure, and copper is still highly soluble without the need for complex coordination chemistry. Fig. 5B shows that, after electrodeposition for the similar time frame as before under the stated conditions, the hexagonal superstructure

is evident in the geometric patches. Electron diffraction studies revealed the presence of crystalline copper (along with cuprous oxide) in the electron dense material seen in the figure, which is evidence of an electrodeposition process as opposed to simple copper staining or complexation with the protein sheets.

#### 4. Conclusions

The ability of the HPI layer of *D. radiodurans* to retain long-range order was investigated over a wide range of pH and following  $1$ – $1000$  s of exposure to the electrolyte. The aim of this study was to develop a rational approach to formulating electrolytes for electrochemical fabrication of dense arrays of nanomaterials. We are well aware that the pH is not the only electrolyte component that can impact protein stability. Thus, while results such as those compiled in Fig. 4 can provide valuable guidance, they do not ensure success. Our results highlight the fact that data from biochemical studies cannot be readily extrapolated to protein-aided electrochemical nanofabrication.

#### Acknowledgments

This work was funded by Genetically Engineered Materials Science and Engineering Center (GEMSEC), a National Science Foundation-Materials Research Science and Engineering Center (NSF-MRSEC) at the University of Washington, Seattle, WA, USA.

#### References

- [1] K. Douglas, G. Devaud, N.A. Clark, *Science* 257 (1992) 642.
- [2] W. Pompe, M. Mertig, R. Kirsch, A.A. Gorbunov, A. Sewing, H. Engelhardt, A. Mensch, *Proc. SPIE* 2779 (1996) 72.
- [3] W. Shenton, D. Pum, U.B. Sleytr, S. Mann, *Nature* 389 (1997) 585.
- [4] M. Mertig, R. Kirsch, W. Pompe, H. Engelhardt, *Eur. Phys. J. D* 9 (1999) 45.
- [5] S.R. Hall, W. Shenton, H. Engelhardt, S. Mann, *Chem. Phys. Chem.* 2 (2001) 184.
- [6] R. Wahl, M. Mertig, J. Raff, S. Selenska-Pobell, W. Pompe, *Adv. Mater.* 13 (2001) 736.
- [7] L. Malkinski, R.E. Camley, Z. Celinski, T.A. Winningham, S.G. Whipple, K. Douglas, *J. Appl. Phys.* 93 (2003) 7325.
- [8] D.B. Allred, M. Sarikaya, F. Baneyx, D.T. Schwartz, *Nano Lett.* 5 (2005) 609.
- [9] S.S. Mark, M. Bergkvist, X. Yang, L.M. Teixeira, P. Bhatnagar, E.R. Angert, C.A. Batt, *Langmuir* 22 (2006) 3763.
- [10] U.B. Sleytr, P. Messner, D. Pum, M. Sára, *Crystalline Bacterial Cell Surface Proteins*, Academic Press, Austin, TX, 1996.
- [11] H. Engelhardt, J. Peters, *J. Struct. Biol.* 124 (1998) 276.
- [12] P. Lancy Jr., R.G.E. Murray, *Can. J. Microbiol.* 24 (1978) 162.
- [13] W. Baumeister, F. Karrenberg, R. Rachel, A. Engel, B. Ten Heggeler, W.O. Saxton, *Eur. J. Biochem.* 125 (1982) 535.
- [14] W. Baumeister, O. Kübler, H.P. Zingsheim, *J. Ultrastruct. Res.* 75 (1981) 60.
- [15] D.E. Garfin, *Methods Enzymol.* 182 (1990) 425.
- [16] B. Emde-Kamola, F. Karrenberg, *FEMS Microbiol. Lett.* 42 (1987) 69.
- [17] M.M. Bradford, *Anal. Biochem.* 72 (1976) 248.